HYDROLOGICAL PROCESSES
Hydrol. Process. (2014)
Published online in Wiley Online Library
(wileyonlinelibrary.com) DOI: 10.1002/hyp.10184

Snow water equivalent time-series forecasting in Ontario, Canada, in link to large atmospheric circulations

Ali Sarhadi,[1]* Richard Kelly[2] and Reza Modarres[3]

[1] *Department of Civil and Environmental Engineering, University of Waterloo, Waterloo, Ontario, Canada, N2L-3G1*
[2] *Department of Geography and Environmental Management, University of Waterloo, Waterloo, Ontario, Canada, N2L-3G1*
[3] *Institute National de la Recherche Scientifique, 490 rue de la couronne, Québec, Québec, Canada, G1K 9A9*

Abstract:

The present study applies different time-series models for forecasting daily and monthly snow water equivalent (SWE) data in Ontario, Canada, during 1987–2011. For daily time series, which showed a significant negative trend, four categories of the autoregressive moving-average (ARMA) and ARMA model with exogenous variables (ARMAX) were applied. The North Atlantic Oscillation, Southern Oscillation Index and Pacific/North American Pattern, as large-scale atmospheric anomalies, as well as temperature time series are considered as exogenous variables for ARMAX models. According to the multicriteria performance evaluation, a time-trend ARMAX model demonstrated the best performance for modelling and forecasting daily SWE. Two models, seasonal autoregressive integrated moving average (SARIMA) and SARIMA with exogenous variables (SARIMAX), were also fitted to the monthly SWE time series. The results revealed that the SARIMAX model showed a better performance than the SARIMA model according to multicriteria evaluation. The three nonparametric tests, Wilcoxon, Levene and Kolmogorov–Smirnov for forecasting evaluation demonstrated that the selected time-series models had enough reliability for short-term SWE forecasting in Ontario. The results of this study also demonstrate the importance of incorporating both trend and appropriate exogenous variables for SWE time-series modelling and forecasting. Copyright © 2014 John Wiley & Sons, Ltd.

KEY WORDS time-series forecasting; snow water equivalent; time-trend ARMAX; SARIMAX; Ontario

Received 26 June 2013; Accepted 24 February 2014

INTRODUCTION

Snowmelt runoff is considered as one of the main sources of surface water supply in mid-latitude to high-latitude river catchments and has a key role in regional-scale water resources management (McNamara *et al.*, 1998; Dery *et al.*, 2005). From a hydrological point of view, snow water equivalent (SWE) is the total water stored in a snowpack that is available when the pack melts. Therefore, SWE forecasting can help water resources authorities define accurate water operating policies for effective water management, such as reservoir flow regulation, agricultural surface water allocation and hydropower generation scheduling. Hence, the accuracy of SWE forecasting has a significant effect on the operation efficiency of the water resources systems (Karamouz and Zahraie, 2004).

In the past decades, many researchers have developed statistical methods to model behaviour of hydroclimatic time series affected by stochastic periodic components. Autoregressive moving-average (ARMA) time-series models developed by Box and Jenkins (1976) have been a common approach among hydrologists for modelling and forecasting time-varying statistical characteristics of hydroclimate variables (Salas *et al.*, 1980; Hipel and McLeod, 1994). Different studies have used the ARMA model and its extensions, such as autoregressive integrated moving-average (ARIMA), seasonal ARIMA (SARIMA) and ARMA with exogenous variable (ARMAX) models, for modelling and forecasting hydrological and climatological variables such as precipitation (Soltani *et al.*, 2007), drought (Mishra and Desai, 2005) and stream flow (Modarres, 2007). However, very few applications of ARMA models have been developed for SWE modelling and forecasting. For example, Haltiner and Salas (1988) used ARMAX for forecasting daily stream flow resulting from snowmelt and rainfall in the Rio Grande River in southern Colorado and reported improved flow forecasts with fewer model parameters. However, the emphasis in this study was on stream flow forecasting and not on SWE prediction.

The aim of this study is to develop different types of ARMA models for daily and monthly SWE time-series forecasting in Ontario. In addition, the present study

*Correspondence to: Ali Sarhadi, Department of Civil and Environmental Engineering, University of Waterloo, Waterloo, Ontario, Canada N2L-3G1.
E-mail: asarhadi@uwaterloo.ca

attempts to develop ARMAX models with exogenous variables such as a number of large-scale atmospheric low-frequency variability modes and local observed meteorological data, for SWE time-series forecasting.

The next section provides the proposed methods for SWE time-series forecasting. The methods are followed by an illustrative example of 24 years of daily and monthly satellite-based SWE time-series modelling for Ontario, Canada. The results section presents the key findings, and the last section discusses the significance of the results, concluding with recommendations for future studies.

METHODOLOGY

Time-series models

To analyse stochastic characteristics of the hydroclimatic time series, the general time-series model is described by a multiplicative SARIMA$(p, d, q)\times(P, D, Q)_s$ model, which is shown in the following form:

$$\phi_p(B)\Phi_P\left(B^S\right)\nabla^d\nabla_S{}^D Y_t = \theta_q(B)\Theta_Q\left(B^S\right)a_t \qquad (1)$$

where Y_t is the observed time series, $\phi_p(B)$ is a polynomial of order p, $\theta_q(B)$ is a polynomial of order q, ∇^d is the nonseasonal differencing operator, B is the backward operator, Φ_P and Θ_Q are the seasonal polynomials of orders P and Q, ∇_S^D is the seasonal differencing operators, S represents the seasons and a_t is an independent identically distributed normal error with a zero mean and standard deviation σ_a.

The following equations give the nonseasonal and seasonal differencing operators, which are selected to be just large enough to remove all nonseasonal and seasonal nonstationarity:

$$\nabla^d Y_t = (1-B)^d Y_t \quad \text{and} \quad B^d Y_t = Y_{t-d} \qquad (2)$$

$$\nabla_S{}^D Y_t = \left(1-B^S\right)Y_t \quad \text{and} \quad B^D Y_t = Y_{t-D} \qquad (3)$$

In the multiplicative form of the SARIMA model, the nonseasonal and seasonal autoregressive operators are multiplied together on the left-hand side while the moving-average operators are multiplied together on the right-hand side (Hipel and McLeod, 1994).

The preceding model is applied in the case of existing seasonality (or significant autocorrelation coefficients at higher seasonal lag times, $k = 12, 24, 36, \ldots$). If no seasonality is observed in Y_t, the preceding model reduces to the following ARIMA model:

$$\phi_p(B)\nabla^d Y_t = \theta_q(B)a_t \qquad (4)$$

For those time series that do not show a nonseasonal nonstationarity (or significant autocorrelation coefficients at higher lag times, $k > 7$), the ARIMA model will reduce to an ARMA model, which contains two polynomials of order p and q, as is shown in the following:

$$\phi_p(B)Y_t = \theta_q(B)a_t \qquad (5)$$

The preceding ARIMA and SARIMA models can be used to model a single time series. However, in some situations, we need to predict a hydroclimatic variable by using a number of predictors called 'exogenous variables' through time. This type of model is called an ARMAX model, which can be written as

$$\phi_p(B)Y_t = \omega_s(B)x_t + \theta_q(B)a_t \qquad (6)$$

where ω_s is the parameter of the model and x is the independent variable. This type of model is used in this study for modelling the temporal relationship between an SWE (as an independent variable) and exogenous variables.

Time-series modelling procedure

To establish time-series models, three steps should be followed: model identification, parameter estimation and goodness-of-fit test. These three steps are described briefly in the following sections (Hipel and McLeod, 1994).

Model identification. The purpose of the identification step is to represent the behaviour of the time series, and to determine if the series is nonseasonal or seasonal and the order of both seasonal and nonseasonal parameters (P, Q, p and q).

To identify the order of the model, the autocorrelation function (ACF) and partial ACF (PACF) are used, both of which measure the amount of a linear dependence among observations separated by k time lags and residuals of time series. The presence of nonstationarity in the series and a cyclic behaviour produced by seasonality can be virtually detected using ACF and PACF. If the autocorrelation coefficients are significant for large lag times (usually $k > 7$–10), the series is assumed nonstationary in time. On the other hand, if the autocorrelation coefficients are significant at lags $k = 12, 24, 36, \ldots$, it is said that the time series has a seasonal variation and nonstationary. A nonseasonal or seasonal differencing operator is used to convert a nonstationary series to a stationary time series.

Model estimation. The next step after identifying an initial model in the first step is the efficient estimation of the model's parameters. The parameters should satisfy two conditions, stationarity and invertibility, for the autoregressive and moving-average models (Box and Jenkins, 1976; Salas *et al*., 1980). The parameters that are

estimated by statistical methods such as the method of moments or the method of maximum likelihood should also be statistically significant. If the model's parameters satisfy the preceding conditions, they are kept in the model, and the model's adequacy is then checked in the next step. Otherwise, the order of the initial candidate model should be changed, and its parameters should satisfy the adequate order of parameters and their significant estimates.

Model diagnostic checking. Model diagnostic checking or goodness-of-fit testing includes testing for autocorrelation in the residuals of the model. In other words, a model should have time independent and normally distributed residuals to be considered adequate. In this study, two methods are applied to test the nonexistence of time independence in the structure of the model residuals. A simple method is an inspection of the ACF of the residuals (or PACF). The lag k autocorrelation coefficients of the residuals of an independent series of length of n are assumed to be normally distributed with a mean of zero and a variance of $1/n$. The 95% confidence limits are given by $\pm 1.96/\sqrt{n}$. The validity of a time-series model is accepted if all autocorrelation coefficients fall within the confidence limit.

The other common test used to test time independence and normality of the residuals is the Ljung–Box lack-of-fit test (Box and Jenkins, 1976). This test, more formally, the Portmanteau lack-of-fit test, computes a statistic, Q, which is approximately distributed as $\chi^2(L-p-q)$ and is given by

$$Q = N(N+2)\prod_{i=1}^{L}(N-k)^{-1}r_k^2(\varepsilon) \tag{7}$$

where N is the sample size and L is the number of autocorrelations of the residuals included in the statistic. L can vary between 15 and 25 for nonseasonal models and $2S$ and $4S$ for seasonal models (Hipel and McLeod, 1994). r_k is the sample autocorrelation of the residual time series, ε, at lag k. If the probability of Q is less than $\alpha = 0.01$, there is strong evidence that the residuals are time dependent and the model is inadequate. If this probability is higher than $\alpha = 0.05$, it is reasonable to conclude that the residuals are time independent and the model is adequate.

Time-series modelling in the presence of trend

The ARMA model has a key assumption: stationarity of the statistical moments through time or trend-free time series. Therefore, before applying ARMA models, it is necessary to check the trend in the SWE time series. For this purpose, the Mann–Kendall test is applied (Mann, 1945; Kendall, 1975).

For a sample of size n, $x_1, \ldots, x_n$, the null hypothesis is that the sample is independent and identically distributed, and the alternative hypothesis of a two-sided test is that the distributions of x_i and x_j are not identical. The Mann–Kendall test statistic based on test statistic S is therefore defined as follows:

$$S = \sum_{i=1}^{n}\sum_{j=1}^{i-1}\operatorname{sign}(x_i - x_j) \tag{8}$$

The mean and the variance of S are written as follows:

$$E[S] = 0 \tag{9}$$

$$\operatorname{var}[S] = \frac{n(n-1)(2n+5) - \sum_{p}^{q} t_p(t_p-1)(2t_p+5)}{18} \tag{10}$$

where t_p is the number of ties for the pth value and q is the number of tied values. The standardized test statistic (Z_{MK}) is computed by

$$Z_{\mathrm{MK}} = \begin{cases} \dfrac{S-1}{\sqrt{\operatorname{Var}(s)}} & S > 0 \\ 0 & S = 0 \\ \dfrac{S+1}{\sqrt{\operatorname{Var}(s)}} & S < 0 \end{cases} \tag{11}$$

A positive Z_{MK} indicates an increasing trend, while a negative Z_{MK} demonstrates a negative trend.

In the event of a significant trend in SWE time series, we first remove it using a linear regression model between SWE and time. The time-series models, ARMA or ARMAX, are then fitted to the residuals of the linear model, which are now trend-free time series. In other words, a time-trend ARMA or ARMAX model (TT-ARMA or TT-ARMAX, respectively) captures both deterministic and stochastic parts of the fluctuations of a time series (Modarres *et al*., 2012).

Model performance

In order to evaluate the performance of the different models, in terms of agreement between observed and model-predicted data, the following criteria are used in this study:

- Correlation coefficient between observed and predicted series.
- Model efficiency (E):The model efficiency criterion, proposed by Nash and Sutcliffe (1970), for model evaluation is written as

$$E = 1 - \frac{\sum(O_i - F_i)}{\sum(O_i - \overline{O})} \tag{12}$$

where E is the coefficient of efficiency, O_i is the observed SWE, F_i is the predicted SWE and $\overline{O}$ is the average of the observed SWE time series. A value of 90% or above indicates satisfactory performance for the model, a value between 80% and 90% is fairly good performance and a lower value is a questionable fit.

- Root mean squared error:

$$RMSE = \left(\frac{\sum_{i=1}^{n}(F_i - O_i)}{n}\right)^{0.5} \tag{13}$$

where O_i and F_i are the observed and predicted SWE data.

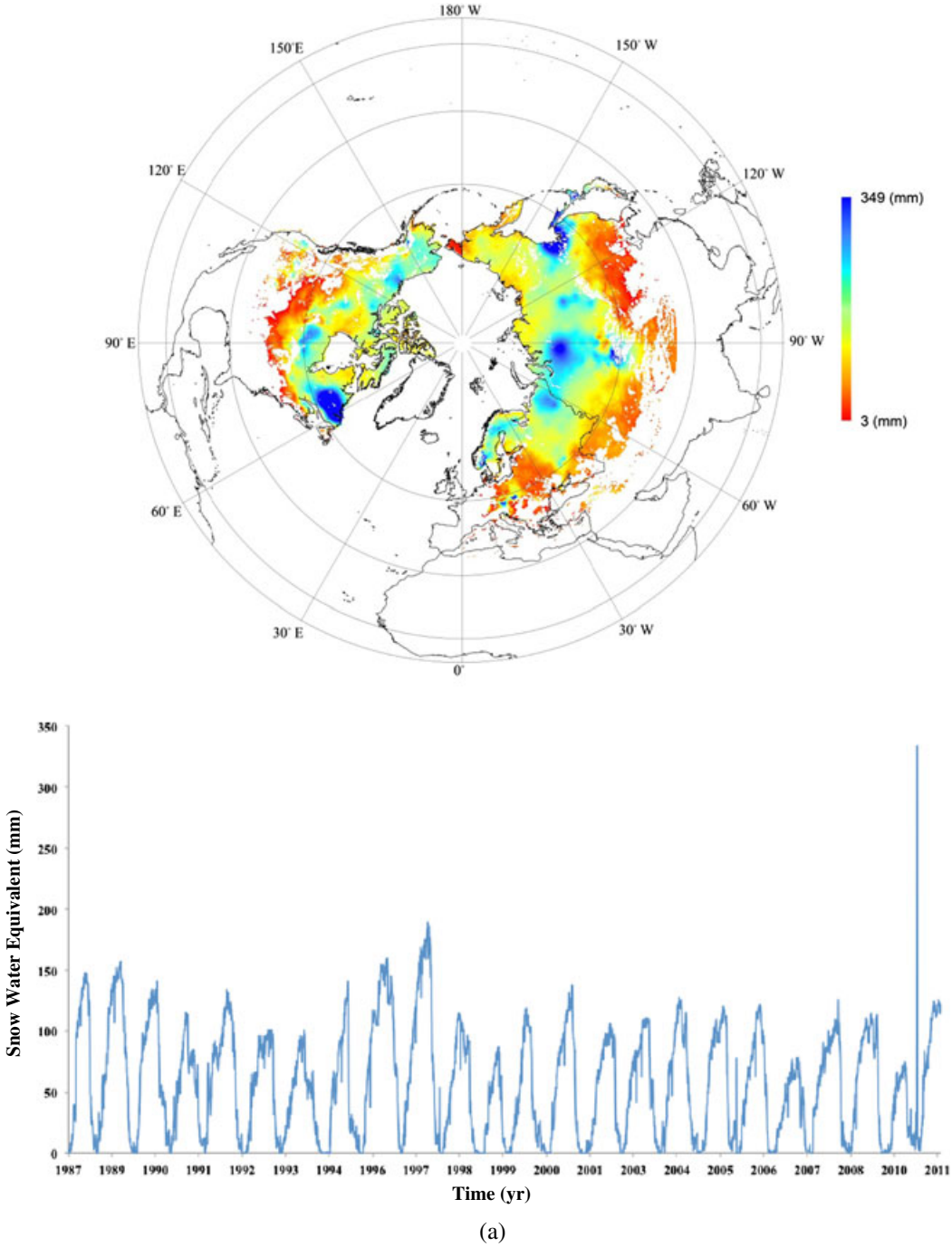

(a)

Figure 1. (a) Daily time series of the snow water equivalent (SWE) data, and an example of the daily SWE product of the European Globe Space Agency (ESA) GlobSnow data for 21 January 2006. (b) Monthly time series of the SWE data, and an example of the monthly product of the ESA GlobSnow data for January 2006

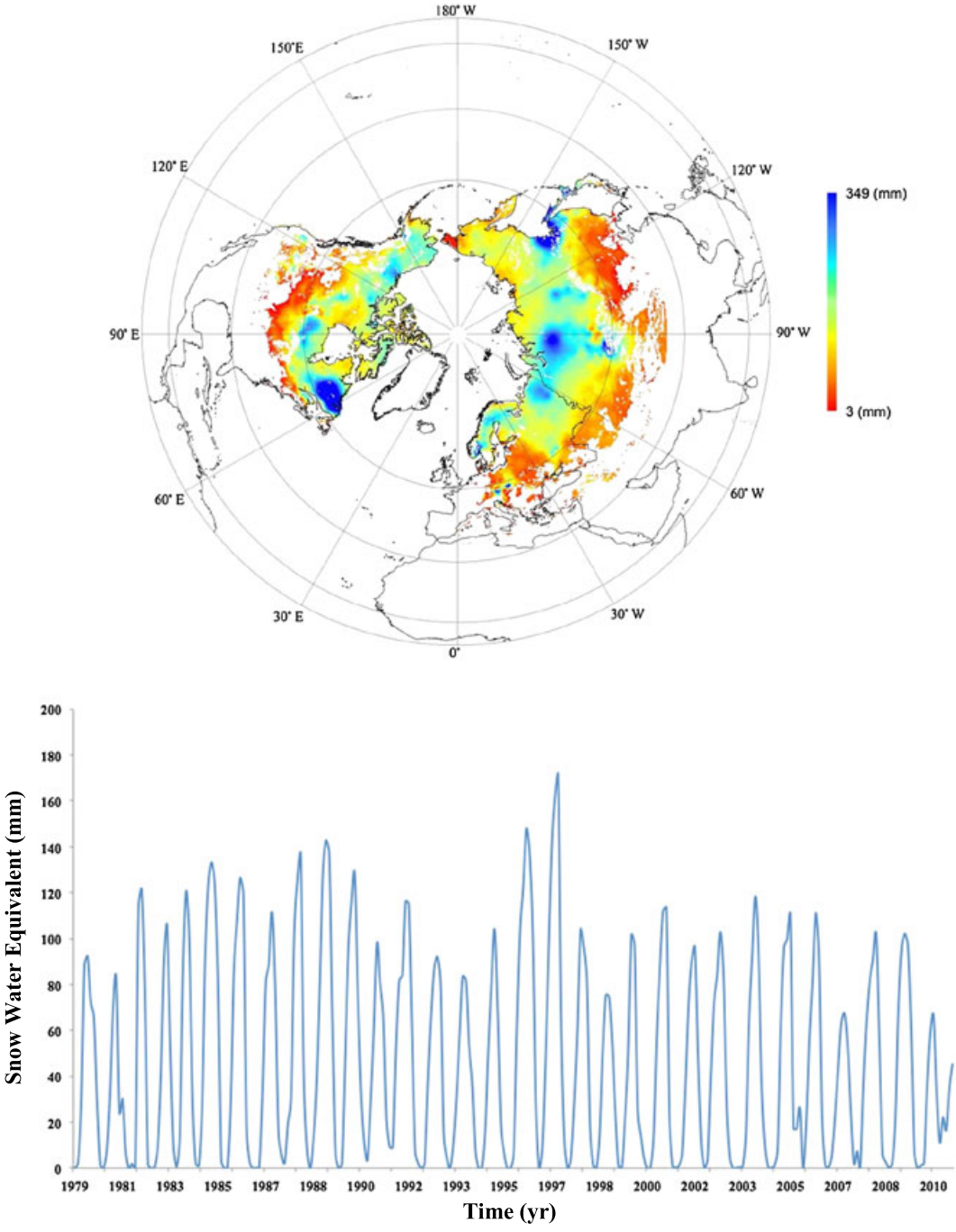

(b)

Figure 1. Continued

Besides the preceding modelling performance criteria, the performance of the selected models for out-of-sample SWE forecasting is also investigated. We use the selected time-series models for 1-month-ahead daily SWE and 6-months-ahead monthly SWE time-series forecasting. In this regard, three nonparametric tests are applied to evaluate the performance of the models for out-of-sample SWE forecasting. These nonparametric criteria are Kolmogorov–Smirnov test for testing the equality of the cumulative distribution function, Wilcoxon rank sum test for equality of the mean and the Levene's test for equality of the variance of out-of-sample forecasted and observed SWE. The reader is referred to Modarres (2007) for more details on these tests.

STUDY AREA AND DATASET

Snow water equivalent data

The main SWE dataset used in this study is derived from European Globe Space Agency GlobSnow products, which produce SWE daily-based, weekly-based and monthly-based data retrieved from SMMR, SSM/I and AMSR-E sensors (Takala *et al.*, 2011). The GlobSnow product uses ground-based weather station observations and passive microwave observations in an assimilation scheme to estimate SWE data for the northern hemisphere, excepting mountainous areas (owing to the uncertainty of microwave measurements, no SWE is retrieved in these areas, although no mountainous terrains exist in Ontario). The spatial resolution of this information is 25 km on EASE-Grid projection and span the period of 1978–2011. In the present study, the daily-based and monthly-based SWE data of Ontario are extracted from GlobSnow products (http://www.globsnow.info/swe).

Figure 1 represents extracted daily and monthly SWE time series from GlobSnow data in Ontario from 1987 to 2011. The data show an annual increase of SWE in the fall of each year, maximum snow in winter and minimum snow in summer. The Province of Ontario, Canada, is selected for a case study because of the important role of snow forecasting in water resources management and economy, particularly in local water consumption, irrigation and hydroelectric power generation.

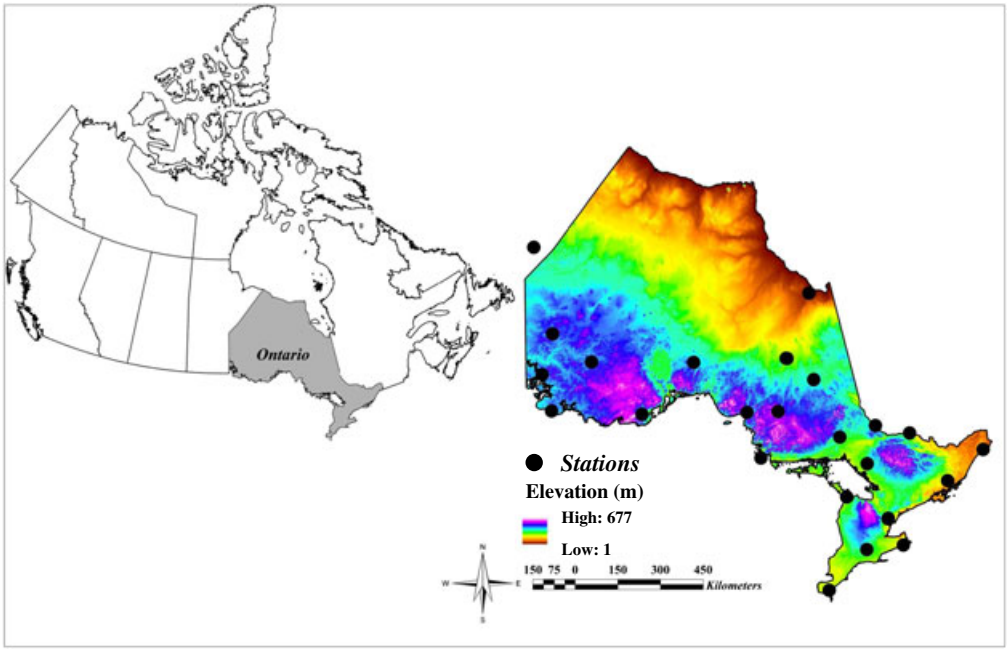

Figure 2. Situation of the study area and location of the meteorological stations across Ontario

Table I. Summary of daily and monthly statistical properties of the SWE data as well as large-scale atmospheric teleconnection patterns for the time period of 1987-2011

Parameters	Data scale	Mean	Standard deviation	Coefficient of variation	Skewness	Kurtosis
SWE (mm)	Daily	57.78	44.93	159.11	0.361	−0.70
	Monthly	46.88	43.72	146.81	0.57	−0.86
Temperature (°C)	Daily	−1.6	10.55	111.5	0.16	−0.75
	Monthly	0.10	9.41	88.57	0.03	−1.14
SOI	Daily	0.05	2.40	5.98	−0.19	−0.30
	Monthly	−0.14	2.69	7.27	−0.09	−0.17
NAO	Daily	0.12	0.83	0.69	−0.22	−0.15
	Monthly	0.07	0.52	0.27	−0.08	−0.35
PNA	Daily	0.099	0.76	0.59	−0.34	−0.11
	Monthly	0.11	0.48	0.23	−0.06	−0.60

NAO, North Atlantic Oscillation; PNA, Pacific/North American Pattern; SOI, Southern Oscillation Index; SWE, snow water equivalent.

Exogenous variables

A number of studies have demonstrated the linkage between snow features and variability of large-scale atmospheric circulation patterns in different parts of Canada. For example, Zhao *et al*. (2013) studied the relationship of the Pacific/North American Pattern (PNA) and North Atlantic Oscillation (NAO) to the annual maximum SWE (SWE_{max}) anomalies over southern parts of Canada. They found that SWE_{max} is significantly correlated with the NAO variations in eastern Canada, especially over central Ontario, while the correlation in western Canada is more closely associated with PNA variations. Similar results have also been reported in other studies of snow cover (Gutzler and Rosen, 1992; Karl *et al*., 1993; Saito *et al*., 2004; Brown, 2010).

Therefore, in this study, we apply three main large-scale atmospheric indices, PNA, NAO and Southern Oscillation Index (SOI), together with temperature as the exogenous variable for SWE time-series modelling and forecasting.

Daily indices of the NAO and PNA are obtained from the Climate Prediction Center, NOAA/National Weather Service (ftp://ftp.cpc.ncep.noaa.gov/cwlinks/), and values of the SOI (obtained from http://www.cpc.ncep.noaa.gov/data/indices/soi) are converted into a daily scale by using a linear interpolation approach to produce daily SOI values for comparing the indices in the same scale (Rasouli *et al*., 2012). To evaluate the monthly variations of the NAO and PNA indices, a monthly time series is formed using an average function, which measures the central tendency of the daily indices. In addition, in order to evaluate the effect of local recorded meteorological factors on the SWE data, mean temperatures from 24 meteorological stations distributed across Ontario

Table II. Pearson correlation coefficients between the daily and monthly SWE data and climatic indices

SWE	Temperature	PNA	NAO	SOI
Daily based	−0.334**	0.019	0.213**	−0.070**
Monthly based	−0.832**	0.127*	0.268**	−0.034

NAO, North Atlantic Oscillation; PNA, Pacific/North American Pattern; SOI, Southern Oscillation Index; SWE, snow water equivalent.
**$p < 0.01$;
*$p < 0.05$.

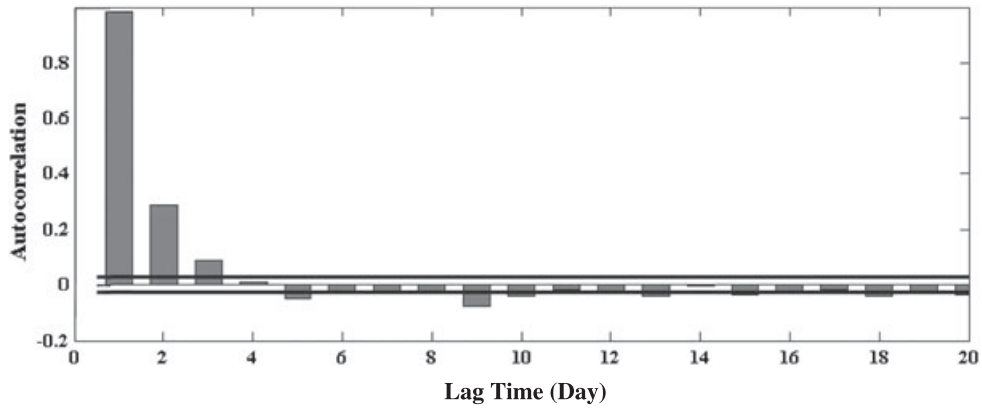

Figure 3. Autocorrelation function of the nonseasonal daily time series of the snow water equivalent (solid lines show confidence levels)

Table III. Multicriteria comparison of the best selected models for the daily snow water equivalent time series

Group	Models	Exogenous variables	R^2	RMSE	MAE	IoAd	CE
1	ARMA(1, 1)	—	0.956	8.53	7.80	0.71	0.968
2	TT-ARMA(1, 1)	—	0.968	8.02	3.90	0.89	0.967
3	ARMAX(1, 1)	Temperature	0.968	8.02	3.90	0.85	0.968
		NAO	0.983	5.93	3.62	0.97	0.983
		SOI	0.983	5.94	3.69	0.96	0.981
		PNA	0.968	8.02	3.90	0.87	0.968
		NAO, SOI, PNA, temperature	0.983	5.91	3.61	0.98	0.983
4	TT-ARMAX(1, 1)	NAO, SOI, PNA, temperature	0.984	5.92	3.61	0.99	0.985

ARMA, autoregressive moving-average model; ARMAX, autoregressive moving-average model with exogenous variables; CE, coefficient of efficiency; IoAd, index of agreement; MAE, mean absolute error; NAO, North Atlantic Oscillation; PNA, Pacific/North American Pattern; RMSE, root mean square error; SOI, Southern Oscillation Index; SWE, snow water equivalent; TT, time trend.

(Figure 2) are applied at two timescales: daily and monthly. The variables are assembled for the 1987–2011 period.

After extraction of the daily time series from GlobSnow data, SWE data are converted into monthly-based data by using the average of the daily data for each month. The statistical characteristics of the two SWE time series (daily and monthly), the atmospheric teleconnection patterns (NAO, PNA and SOI) and *in situ* surface air temperature data are shown in Table I.

Table II also shows the association of the large-scale atmospheric patterns and local observed data (temperature) with the daily SWE series. A significant negative correlation at the 1% level ($P < 0.01$) is found between temperature and SOI and the daily SWE series, while NAO shows a positive correlation at the 1% significant level with daily SWE. The PNA index has also a positive correlation with daily SWE, although it is not statistically significant.

Table IV. Estimated parameters for the TT-ARMAX(1, 1) for daily time series

Parameters	Coefficient	Standard error	*t*-ratio	$P < 0.01$
ϕ_1	0.98	0.002	328.2	0.0001
θ_1	−0.08	0.015	−5.38	0.0001

RESULTS

Daily time-series modelling

For the first step or model identification, we check the ACF of the daily SWE series (Figure 3). According to the ACF,

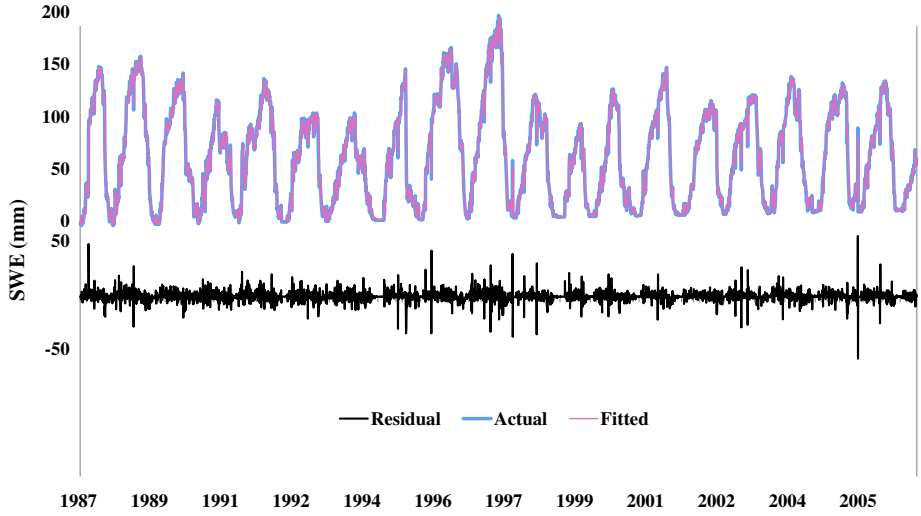

(a)

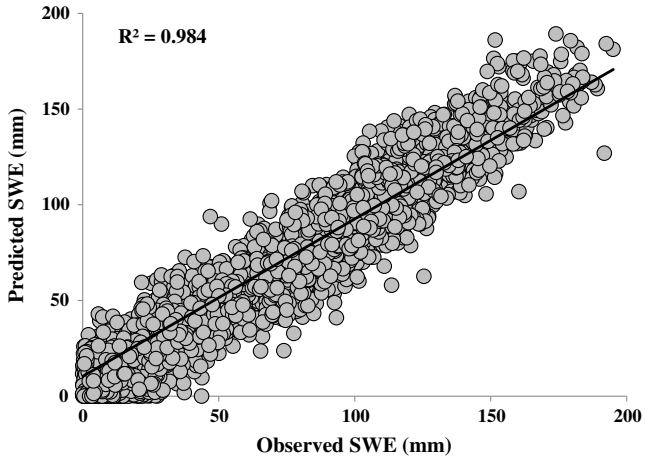

(b)

Figure 4. (a) Observed and modelled daily snow water equivalent (SWE) data, (b) performance of the best selected model (TT-ARMAX(1, 1))

autocorrelation coefficients of the first three lags are significant, and the rest fall within the confidence level and are not significant. It is apparent that the ACF of the daily series demonstrates no seasonal variations among these data as the autocorrelation coefficients are not significant at lag times $k = 12, 24, 36, \ldots$. Therefore, a nonseasonal ARMA(1, 1) model and a nonseasonal ARMAX(1, 1) model are appropriate options to model time series in order to incorporate the effect of atmospheric indices in time-varying SWE.

Trend analysis is applied to check the nonstationarity of the daily SWE time series. The result of the Mann–Kendall test shows a decreasing trend at the 1% significant level for the daily SWE time series. It should be noted that Takala *et al*. (2011) also showed a significant negative trend for SWE data in the whole hemisphere. After removing this trend from daily SWE data by a simple linear regression model between SWE and time, a nonseasonal ARMA and ARMAX models are fitted to the trend-free residuals of the regression model. These models are called TT-ARMA and TT-ARMAX. Four nonseasonal models are fitted to daily SWE time series. These models are ARMA(1, 1), TT-ARMA(1,1) without exogenous variables and ARMAX(1, 1) and TT-ARMAX(1, 1) models with various exogenous variables.

The model parameters are estimated using the maximum likelihood method. The ACFs of these models' residuals show that all these models pass the adequacy criteria. To select the best model for daily SWE time-series modelling, the performances of these models are evaluated on the basis of the proposed criteria (Table III).

For the time-series models without exogenous variables, ARMA(1, 1) and TT-ARMA models are compared. According to the coefficient of determination R^2, the TT-ARMA model performs better than the ARMA model. The index of agreement and other error criteria such as the root mean square error and mean absolute error and coefficient of efficiency also show a better performance for the TT-ARMA model. The performance of TT-ARMA is better than that of the ARMA model mainly because it considers both trend in daily SWE data (by a linear model) and stochastic variation of the residuals of the SWE time series.

In the case of ARMAX models with different exogenous variables and according to the R^2 criteria, three models with the same measurement ($R^2 = 0.983$) can be chosen with the different exogenous variables. The

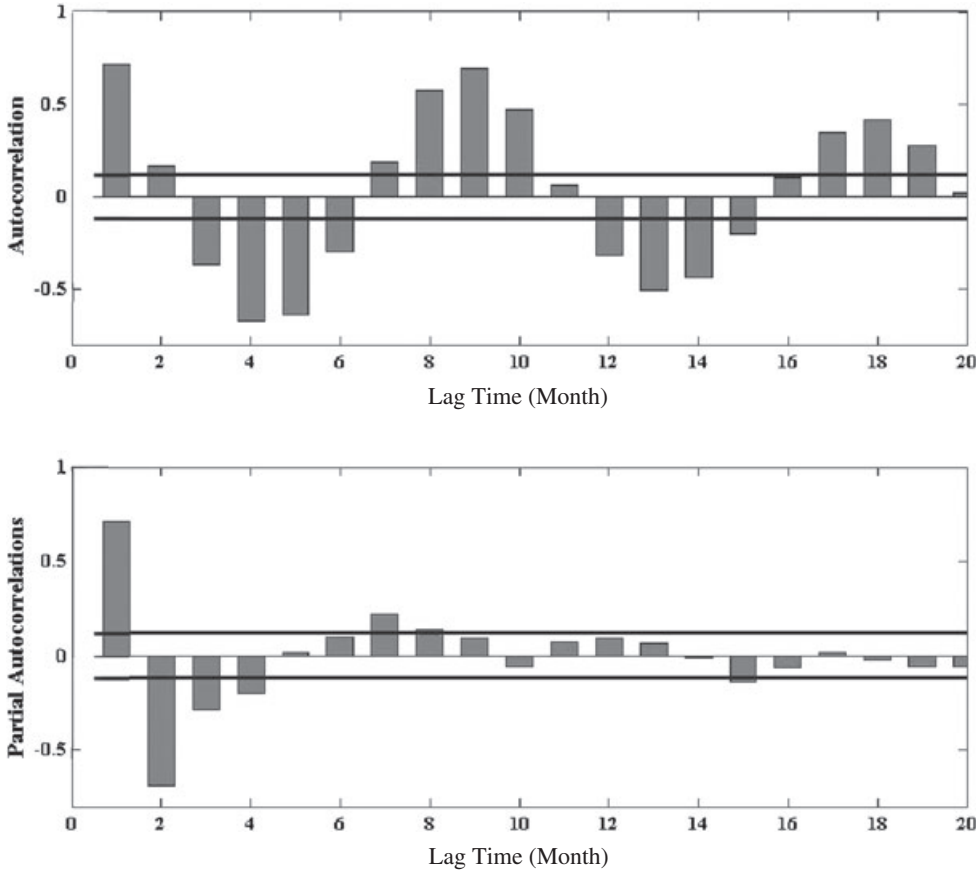

Figure 5. Autocorrelation and partial autocorrelation functions of the seasonal monthly time series of the snow water equivalent (solid lines show confidence levels)

index of agreement measure and error criteria demonstrate that the ARMAX model with a combination of all the independent variables has a slightly better performance than the alternative models. Typically, in the case of having similar models and similar performances, the model with the least parameters is selected as the best model (Haltiner and Salas, 1988). The ARMAX (1, 1) model with only one exogenous variable (NAO) is selected as the best model.

Comparing the ARMAX model with the trend-free model of TT-ARMAX indicates that the approach for modelling daily SWE time series in the presence of a significant trend, TT-ARMAX (1, 1), performs better than the ARMAX(1, 1) model. Table IV presents parameters for the selected model. The observed and estimated daily SWE time series (Figure 4a) and the scatter plot between them (Figure 4b) also show the good performance of the TT-ARMAX model.

Monthly SWE time-series modelling

In order to model the monthly SWE time series, the same methodology as the daily time series is followed. First, the Mann–Kendall test shows no significant trend for monthly SWE time series. The behaviour of the monthly SWE time series is interpreted using ACF and PACF. Figure 5 shows a seasonal variation in the monthly time-series data, as the significant correlation coefficients in the ACF and PACF. Therefore, the SARIMA models are fitted to the monthly series. To find the best SARIMA models, the time independence and normality of the models' residuals are tested by the Portmanteau lack-of-fit test and ACF of residuals, respectively. The results

Table V. Multicriteria comparison of the best selected models for the monthly snow water equivalent time series

Group	Models	Exogenous variables	R^2	RMSE	MAE	IoAd	CE
1	SARIMA(1, 0, 4)(9, 1, 9)$_4$	—	0.915	20.71	17.41	0.98	0.916
2	SARIMAX(1, 0, 4)(9, 1, 4)$_4$	NAO, PNA, temperature	0.919	18.71	16.41	0.99	0.923

CE, coefficient of efficiency; IoAd, index of agreement; MAE, mean absolute error; NAO, North Atlantic Oscillation; PNA, Pacific/North American Pattern; RMSE, root mean square error; SARIMA, seasonal autoregressive integrated moving-average model; SARIMAX, seasonal autoregressive integrated moving-average model with exogenous variables.

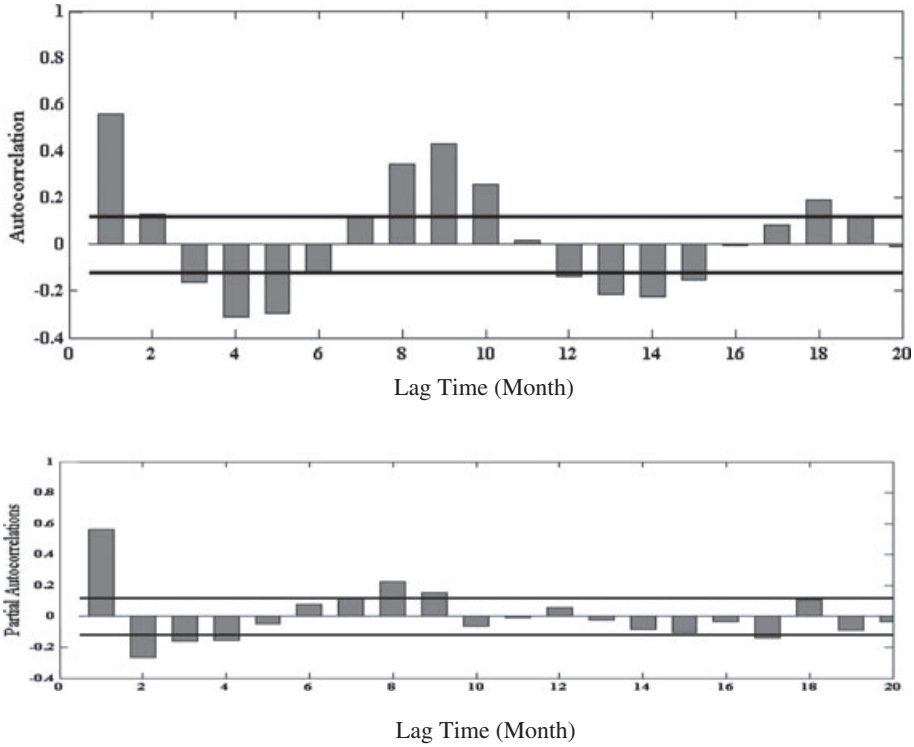

Figure 6. Autocorrelation and partial autocorrelation functions of the seasonal residuals of a multivariate regression model (in which the monthly snow water equivalent time series is the dependent variable and exogenous variables are independent variables)

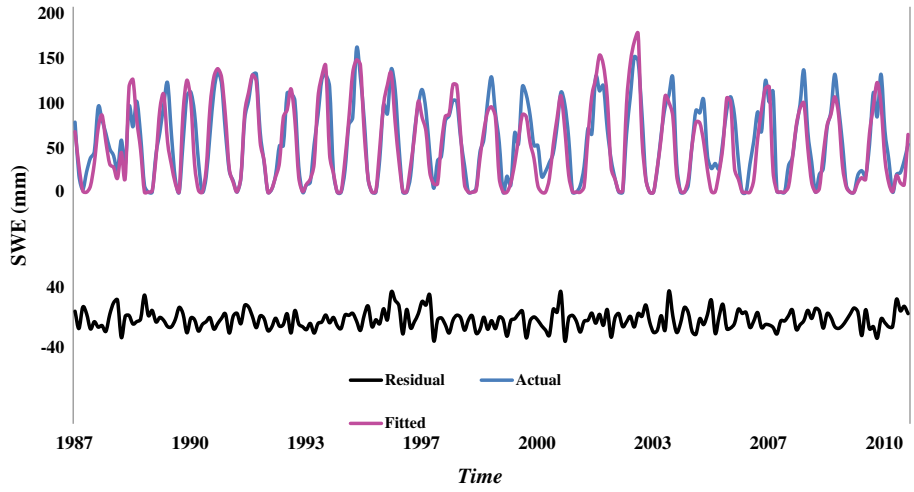

(a)

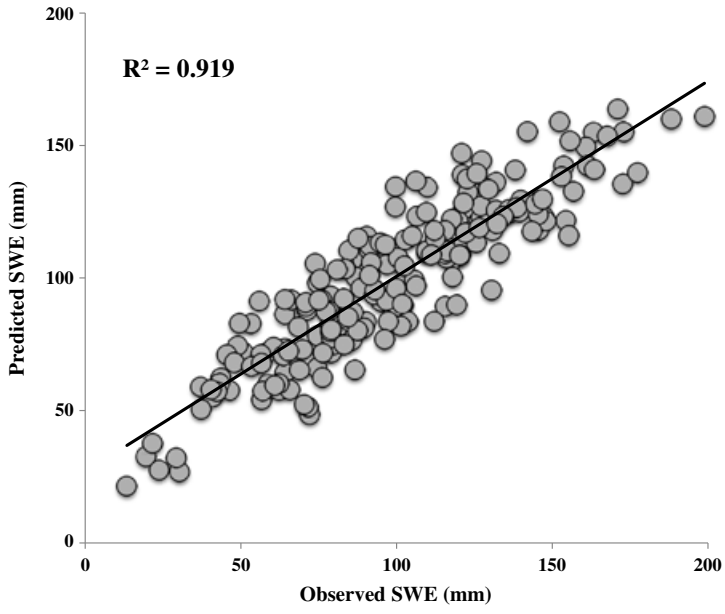

(b)

Figure 7. (a) Observed and modelled monthly snow water equivalent (SWE) data, (b) performance of the best selected model (SARIMAX(1, 0, 4)(9, 1, 4)$_4$)

indicate that SARIMA(1, 0, 4)(9, 1, 9)$_4$ is the best-fitted model among the different potential models (Table V).

To explore the efficacy of including exogenous variables, we use ARMAX models developed by the significant correlated exogenous variables (atmospheric anomaly indices of PNA and NAO and local temperature observations given in Table II) to test the performance of these types of models for forecasting the monthly SWE data. In doing so, a multivariate regression model is developed, in which the monthly SWE series is a dependent variable and the exogenous variables are considered to be independent variables. The ACF and PACF of the residuals of the regression model illustrated in Figure 6 show that residuals follow a seasonal behaviour. Therefore, a SARIMAX(1, 0, 4)(9, 1, 4)$_4$ model is fitted to the residuals of the regression model. To select the best models for forecasting the monthly

Table VI. Estimated parameters for the for SARIMAX(1, 0, 4)(9, 1, 4)$_4$ model for monthly snow water equivalent time series

Parameters		Coefficient	Standard error	t-ratio	$P < 0.01$
Nonseasonal	ϕ_1	0.370	0.098	3.77	0.0001
	θ_4	−0.267	0.102	−2.61	0.0001
Seasonal	Φ_9	−0.225	0.061	−3.70	0.0001
	Θ_4	0.963	0.018	51.86	0.0001

SWE time series, performance criteria are assessed. Results of the performance analysis (given in Table V) reveal that SARIMAX$(1, 0, 4)(9, 1, 4)_4$ represents a better performance than the SARIMA$(1, 0, 4)(9, 1, 9)_4$ model. The time series of the observed and predicted values of the monthly SWE time series for the best model, as well as their scatter plot, are given in Figure 7. The parameters of the selected model are also given in Table VI. The results demonstrate that the prediction ability of SARIMAX models is higher than that of SARIMA models, as the former incorporates predictor variables (NAO, PNA indices and temperature). Moreover, these two atmospheric low-frequency modes and monthly temperature parameters can be used for monitoring the monthly SWE data anomalies in Ontario. These findings are

Table VII. Test results for comparison between the observed and forecasted daily and monthly snow water equivalent data

Data scale	R^2	Coefficient of efficiency	Root mean square error	Wilcoxon's *P*-value	Levene's *P*-value	Kolmogorov–Smirnov *P*-value
Daily	0.91	0.901	2.52	0.964	0.740	0.943
Monthly	0.89	0.898	3.72	0.467	0.703	0.799

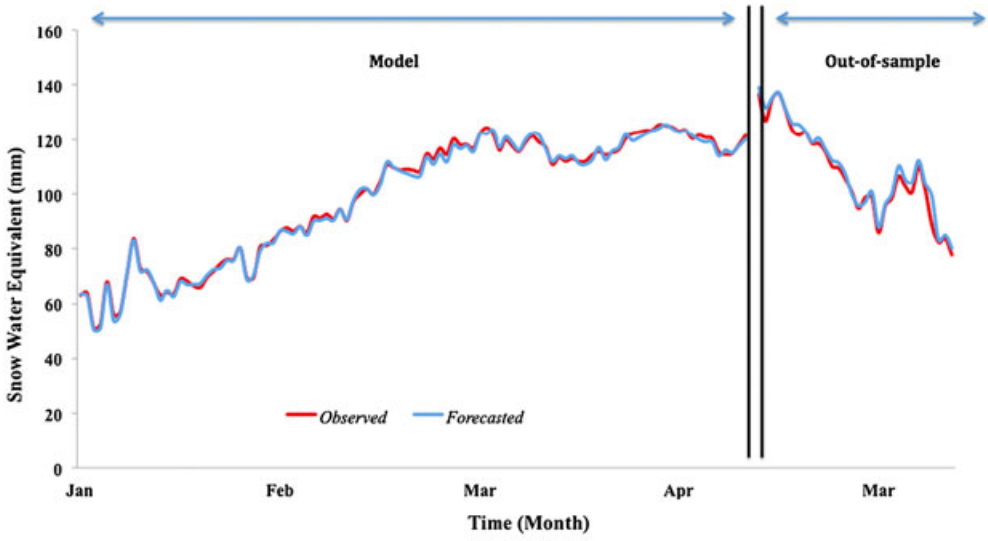

(a)

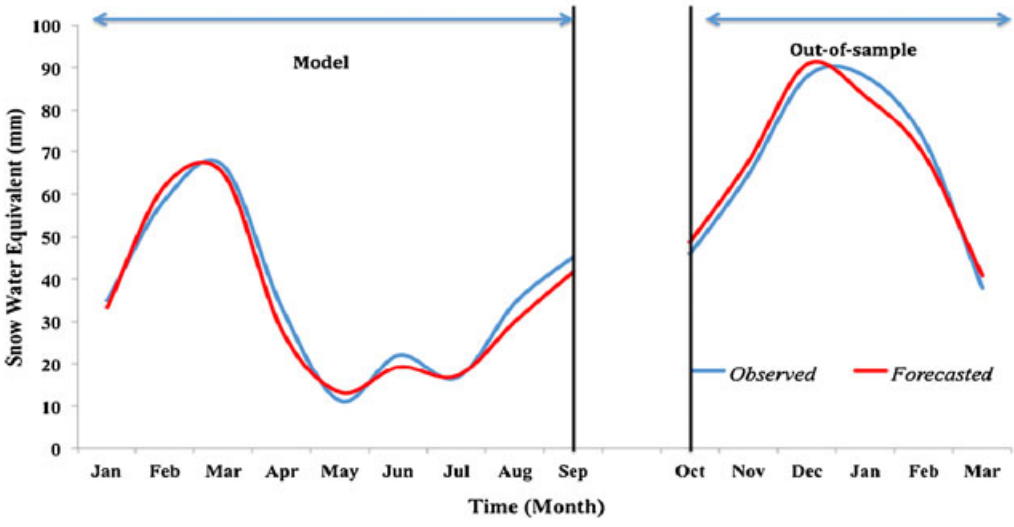

(b)

Figure 8. Comparison of the forecasted and observed snow water equivalent (SWE) data in (a) daily and (b) monthly temporal scales

consistent with the findings of Zhao *et al*. (2013) and Notaro *et al*. (2006) who showed how the combination of the NAO and PNA anomalies affect SWE anomalies and can explain more variance of SWE time-series variation in eastern Canada.

Out-of-sample forecasting

To assess the validity of the best selected models in the previous sections for the two temporal scales, these models are used for out-of-sample daily and monthly SWE forecasting. As time-series modelling is used for forecasting hydroclimatic variables in short-term periods (Haltiner and Salas, 1988), we select a period of 1 month (from 21 April 2011 to 21 May 2011) and a period of 6 months (from December 2010 until May 2011) for forecasting the daily and monthly SWE time series, respectively. The results of the criteria, which are described in the Section on Model Performance and used to compare observed and out-of-sample forecasted SWE time series, are given in Table VII. The results show no significant difference between observed and forecasted SWE time series for both timescales. The correlation coefficient indicates a highly satisfactory forecasting, and the root mean square errors as well as the coefficient of efficiency measurements show a good performance for both temporal scales. The *P*-values of Wilcoxon and Levene, which are larger than 0.05, indicate that there is no difference between the mean and variance of the forecasted and observed SWE time series. In addition, the Kolmogorov–Smirnov criterion demonstrates that there is no difference between distribution functions of the forecasted and observed SWE time series. The results also reveal a slightly better performance of the selected model for SWE daily time series than that for the monthly SWE time series.

The forecasted daily and monthly SWE data and corresponding observed data are illustrated in Figure 8. This figure indicates a good agreement between observed and modelled SWE time series for both time series. The modelled SWE daily time series follows the increasing variation of the observed SWE from January to April in excellent agreement (Figure 8a). In addition, the out-of-sample forecasted SWE time series is well fitted to the observed time series, indicating that the TT-ARMAX performs best for forecasting daily SWE time series. This is mainly due to adding the time trend of SWE and the effect of exogenous variables into the stochastic model.

These conditions are also observed for monthly SWE time-series models (Figure 8b). The estimated SWE time series follows the observed seasonal SWE time series very well from January to September. This very good agreement is also observed between observed and forecasted monthly SWE time series. These results also show the importance of incorporating appropriate exogenous variables for SWE time-series forecasting.

SUMMARY AND CONCLUSION

In the present study, an SWE time series extracted from remotely sensed GlobSnow data is modelled by different time-series approaches in two, daily and monthly, timescales for Ontario, Canada. The most important contribution of this study is the time-series modelling of a daily SWE series in the presence of a trend and the SARIMA modelling of a monthly SWE series. For the daily SWE series, which shows a significant negative trend, four different types of nonseasonal time-series models, namely ARMA, TT-ARMA, ARMAX and TT-ARMAX, are applied to select the best model for predicting the daily SWE data. The results reveal that an ARMA model incorporating both time trend and exogenous variables (i.e. the TT-ARMAX model) for daily SWE time series outperforms the models without trend parameters and atmospheric anomaly variables.

Therefore, this type of ARMAX model is strongly suggested for time-series modelling of the daily and monthly SWE time series and other hydroclimatic variables that have a significant trend. For the seasonal monthly SWE time series, which shows no significant trend, two SARIMA and SARIMAX models are fitted. The multicriteria performance evaluation indicates that incorporating exogenous variables into a SARIMA will improve the performance of the SARIMA model. The results indicate that SWE is more dependent on NAO than on other teleconnection indices (PNA and SOI) and its variation could be used for predicting SWE variations of Ontario. These results are consistent with the study of Zhao *et al*. (2013), which indicates that SWE data are significantly correlated with the NAO index over central Ontario.

The use of the selected model for out-of-sample short-term forecasting suggests that the selected models have a satisfactory validity and are reliable for short-term forecasting the daily and monthly SWE data for Ontario.

It is suggested that the selected models for daily and monthly scales (TT-ARMAX and SARIMAX models) be tested in different regions and, perhaps, for other snow characteristics such as snow cover extent. Taking into account other atmospheric anomaly variables and other temperature parameters such as daily and monthly absolute minimum and maximum temperatures and precipitation for SWE time-series modelling and forecasting is also suggested for future studies. As the selected models are linear and might encompass some inadequacies in performances, application of nonlinear and multivariate time-series models coupled with the exogenous variables applied in this study and other

variables is highly recommended for seasonal and nonseasonal modelling and forecasting of the SWE time series in further studies.

REFERENCES

Box GEP, Jenkins GM. 1976. *Time Series Analysis: Forecasting and Control*, revised edn. Holden Day: San Francisco.

Brown RD. 2010. Analysis of snow cover variability and change in Québec 1948–2005. *Hydrological Processes* **24**(14): 1929–1954.

Dery SJ, Sheffield J, Wood EF. 2005. Connectivity between Eurasian snow cover extent and Canadian snow water equivalent and river discharge. *Journal of Geophysical Resources* **110**: D23106.

Gutzler D, Rosen RD. 1992. Interannual variability of wintertime snow cover across the Northern Hemisphere. *Journal of Climate* **5**: 1441–1447.

Haltiner JP, Salas JD. 1988. Short-term forecasting of snowmelt runoff using ARMAX models. *Journal of the American Water Resources Association* **24**(5): 1083–1089.

Hipel KW, McLeod AE. 1994. *Time Series Modeling of Water Resources and Environmental Systems*. Elsevier: Amsterdam, The Netherlands.

Karamouz M, Zahraie B. 2004. Seasonal streamflow forecasting using snow budget and El Niño-Southern Oscillation climate signals: application to the Salt River Basin in Arizona. *Journal of Hydrologic Engineering* **9**(6): 523–533.

Karl TR, Groisman PY, Knight RW, Heim RRJ. 1993. Recent variations of snow cover and snowfall in North America and their relation to precipitation and temperature variations. *Journal of Climate* **6**: 1327–1344.

Kendall MG. 1975. *Rank Correlation Measures*. Charle Griffin: London, UK.

Mann HB. 1945. Nonparametric tests against trend. *Econometrica* **13**(3): 245–259.

McNamara JP, Kane DL, Hinzman LD. 1998. An analysis of streamflow hydrology in the Kuparuk River Basin, Alaska: a nested watershed approach. *Journal of Hydrology* **206**: 39–57.

Mishra AK, Desai VR. 2005. Drought forecasting using stochastic models. *Stochastic Environmental Research and Risk Assessment* **19**(5): 326–339.

Modarres R. 2007. Streamflow drought time series forecasting. *Stochastic Environmental Research and Risk Assessment* **21**: 223–233.

Modarres R, Ouarda TBMJ, Vanasse A, Orzanco MG, Gosselin P. 2012. Modeling seasonal variation of hip fracture in Montreal, Canada. *Bone* **50**: 909–916.

Nash JE, Sutcliffe JV. 1970. River flow forecasting through. Part I. A conceptual models discussion of principles. *Journal of Hydrology* **10**: 282–290.

Notaro M, Wang WC, Gong W. 2006. Model and observational analysis of the northeast U.S. regional climate and its relationship to the PNA and NAO patterns during early winter. *Monthly Weather Review* **134**: 3479–3505.

Rasouli K, Hsieh WW, Cannon AJ. 2012. Daily streamflow forecasting by machine learning methods with weather and climate inputs. *Journal of Hydrology* **414**: 284–293.

Saito K, Yasunari T, Cohen J. 2004. Changes in the sub-decadal covariability between northern hemisphere snow cover and the general circulation of the atmosphere. *International Journal of Climatology* **24**: 33–44.

Salas JD, Delleur JW, Yevjevich VM, Lane WL. 1980. *Applied Modeling of Hydrologic Time Series*. Water Resources Publications: Littleton.

Soltani S, Modarres R, Eslamian SS. 2007. The use of time series modeling for the determination of rainfall climates of Iran. *International Journal of Climatology* **27**: 819–829.

Takala M, Luojus K, Pulliainen J, Derksen C, Lemmetyinen J, Kärnä J, Koskinen J, Bojkov B. 2011. Estimating northern hemisphere snow water equivalent for climate research through assimilation of space-borne radiometer data and ground-based measurements. *Remote Sensing of Environment* **115**(12): 3517–3529.

Zhao H, Higuchi K, Waller J, Auld H, Mote T. 2013. The impacts of the PNA and NAO on annual maximum snowpack over southern Canada during 1979–2009. *International Journal of Climatology* **33**: 388–395.